

Electronic correlation effects and magnetic properties of $L1_0$ phase of FeNi

A S Belozеров^{1,2}, A A Katanin^{3,2,1}, V I Anisimov^{1,2,4}

¹ Skolkovo Institute of Science and Technology, 121205 Moscow, Russia

² M. N. Miheev Institute of Metal Physics, Russian Academy of Sciences, 620108 Yekaterinburg, Russia

³ Moscow Institute of Physics and Technology, 141701 Dolgoprudny, Russia

⁴ Ural Federal University, 620002 Yekaterinburg, Russia

E-mail: alexander.s.belozеров@gmail.com

Abstract. We study the electronic and magnetic properties of $L1_0$ phase of FeNi, a perspective rare-earth-free permanent magnet, by using a combination of density functional and dynamical mean-field theory. Although $L1_0$ FeNi has a slightly tetragonally distorted fcc lattice, we find that magnetic properties of its constituent Fe atoms resemble those in pure bcc Fe. In particular, our results indicate the presence of well-localized magnetic moments on Fe sites, which are formed due to Hund's exchange. At the same time, magnetism of Ni sites is much more itinerant. Similarly to pure bcc Fe, the self-energy of Fe $3d$ states is found to show the non-Fermi-liquid behavior. This can be explained by peculiarities of density of Fe $3d$ states, which has pronounced peaks near the Fermi level. Our study of local spin correlation function and momentum dependence of particle-hole bubble suggests that the magnetic exchange in this substance is expected to be of RKKY-type, with iron states providing local-moment contribution, and the states corresponding to nickel sites (including virtual hopping to iron sites) providing itinerant contribution.

1. Introduction

Growing demand in recent decades for high-performance permanent magnets and deficiency of rare-earth elements have stimulated an active search of new rare-earth-free magnets. One of the promising materials is ordered $L1_0$ phase of FeNi, which was first discovered in 1962 during the neutron irradiation of disordered FeNi alloy [1]. Later, samples of $L1_0$ FeNi were found in meteorites, and this phase was named tetrataenite after its tetragonal crystal structure and Fe-Ni alloy taenite, also found in meteorites. Formation of tetrataenite in meteorites occurs due to extremely slow cooling (~ 0.1 K per million years) at a temperature of about 600 K. Therefore, an artificial synthesis of its significant amount is challenging. In this respect, a successful fabrication of well-ordered film [2,3] and bulk [4] samples was recently reported.

Tetrataenite has been extensively studied experimentally in the meteorite [5–8] and artificially synthesized [1–4,9–12] samples, that helped to clarify its magnetic properties and their dependence on structural parameters [2,11]. In contrast to the disordered Fe-Ni alloys, tetrataenite can be classified as a hard magnet due to large coercivity of more than 500 Oe [5,6]. Other characteristics of tetrataenite are also comparable to those of rare-earth-based magnets. In particular, it has a high Curie temperature of 823 K [7], a saturation magnetization of ~ 1270 emu/cm³ [9], and the theoretical magnetic energy product of ~ 42 MG Oe [6], which is close to that of Sm-Co and Nd-Fe-B magnets.

The tetragonal $L1_0$ structure of FeNi is of AuCu-type and characterized by chemical ordering, in which Fe and Ni monolayers are alternating along the c -axis (see Fig. 1). Although tetrataenite does not contain heavy elements, such as $4d$ or $5d$ transition metals, the tetragonal distortion serves as a source of large magnetocrystalline anisotropy [9]. The distortion $c/a = 1.007$ in terms of face-centered unit cell parameters is however small; a transformation to body-centered cubic (bcc) lattice requires much smaller $c/a = 1/\sqrt{2}$ in the same notations.

Theoretical studies of $L1_0$ FeNi have been performed mainly within density functional theory (DFT). These studies addressed the origin of magneto-crystalline anisotropy [14] and its dependence on the chemical disorder [15,16], which was shown

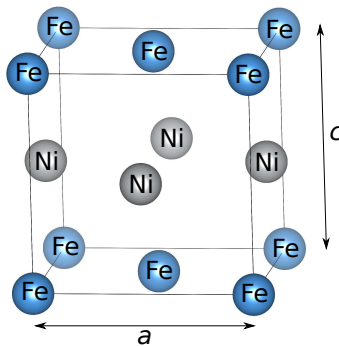


Figure 1. Crystal structure of the $L1_0$ phase of FeNi. The figure was prepared with the VESTA program [13].

to reduce both the Curie temperature and magnetic anisotropy energy (MAE) [16–18]. Interestingly, Izardar *et al* found that certain configurations with partial disorder have a larger MAE than the perfectly ordered $L1_0$ structure [16]. Moreover, the phase stability in FeNi was also considered using DFT calculations [18–20]. In particular, Tian *et al* obtained an accurate estimate of the order-disorder transition temperature and found its strong dependence on the configurational and vibrational degrees of freedom [18].

The DFT alone, however, has difficulties in description of electron correlations, which were shown to play an important role in iron [21–26], nickel [24–26], and their alloys [25–27]. An accurate treatment of local spin dynamics and many-body effects, which can be especially relevant at finite temperatures, is provided by a combination of DFT and dynamical mean-field theory (DMFT) [28]. This combination, called DFT+DMFT [29], was recently applied by Benea *et al* to describe the Compton profile spectra of ferromagnetic $L1_0$ FeNi [30]. This study has demonstrated the limitation of local spin-density approximation in the low momentum region, where the local dynamical correlations were found to be essential for description of the experimental spectra. These results obtained for ferromagnetic state show the importance of further studying the correlation effects in $L1_0$ FeNi, especially above the magnetic transition temperature.

In this paper we explore the electronic and magnetic properties in *paramagnetic* phase of tetrataenite by DFT+DMFT approach. This allows us to trace the presence of well-localized magnetic moments on Fe sites, while we find magnetism of Ni sites is much more itinerant. We also find that electronic and magnetic properties of constituent Fe atoms resemble those in pure bcc Fe, that can be explained by peculiarities of density of Fe 3d states, which has pronounced peaks near the Fermi level.

2. Method and computational details

We employ a fully charge self-consistent DFT+DMFT approach [31] implemented with plane-wave pseudopotentials [32, 33]. The Perdew-Burke-Ernzerhof form of GGA was considered. We adopt the experimental lattice constants $a = b = 3.582$ Å and $c = 3.607$ Å [5], corresponding to the face-centered tetragonal (fct) lattice, with four atoms per unit cell. Nevertheless, our calculations were performed for an equivalent but more compact unit cell of two atoms, that corresponds to a body-centered tetragonal (bct) lattice with $a' = a/\sqrt{2}$ and $c' = c$. The integration in the reciprocal space was carried out using $10 \times 10 \times 10$ \mathbf{k} -point mesh. Our DFT+DMFT calculations explicitly include the 3d, 4s and 4p valence states, by constructing a basis set of atomic-centered Wannier functions within the energy window spanned by the *s-p-d* band complex [34].

We perform DMFT calculations with the Hubbard parameter $U \equiv F^0 = 4$ eV, the Hund's coupling $J_H \equiv (F^2 + F^4)/14 = 0.9$ eV, where F^0 , F^2 , and F^4 are the Slater integrals. These values are in agreement with estimates for elemental iron [35]. We also checked that considering $U = 3$ eV for Ni as well as for both Fe and Ni does not qualitatively affect the results. We use the fully localized double-counting correction,

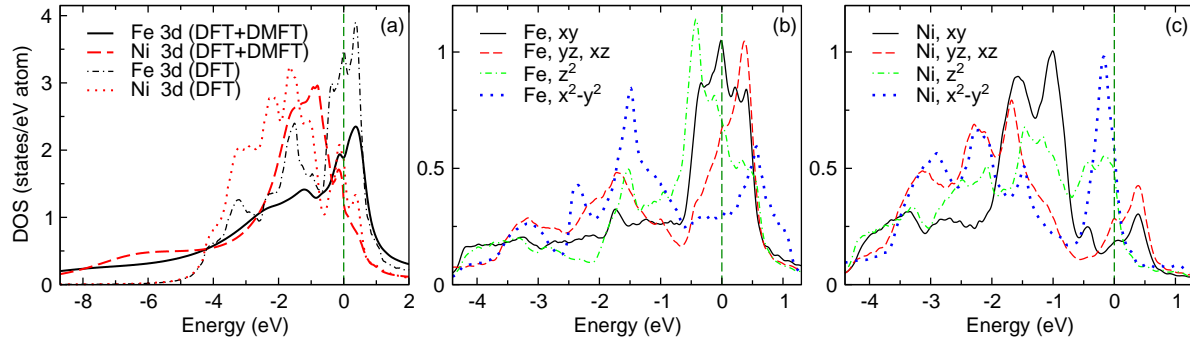


Figure 2. Total (a) and orbital-projected (b,c) density of $3d$ states obtained within DFT (a,b,c) and DFT+DMFT (a) at temperature $T = 1160$ K. The Fermi level is at zero energy.

evaluated from the self-consistently determined local occupations, to account for the electronic interactions already described by DFT. We also verified that the around mean-field form of double-counting correction leads to similar results. The impurity problem was solved by the hybridization expansion continuous-time quantum Monte Carlo method [36] with the density-density form of Coulomb interaction. To compute the density of states, we perform the analytical continuation of self-energies to real-energy range by using the Padé approximants [37].

3. Results and discussion

First we present the density of $3d$ states (DOS) in figure 2(a). Interestingly, the DOS for both constituents shows a significantly different behavior near the Fermi level comparing to pure fcc Fe and Ni. In particular, the DOS for Fe in FeNi has a broad peak in the vicinity of the Fermi level, with a maximum located ~ 0.4 eV above it. The peak resembles that in bcc Fe (see Ref. [21]), where it originates from the e_g states. By contrast, in fcc Fe the peak is much smaller and is located below the Fermi level [38]. The van Hove singularity formed by the t_{2g} states in pure fcc Ni [25] is absent in the DOS of Ni constituent, which has only a small peak at ~ 0.2 eV below the Fermi level. At the same time, a satellite structure at about -6 eV, observed experimentally in pure Ni [39], is also present in $L1_0$ FeNi. In both materials, the DFT alone does not reproduce this satellite originating from many-body effects.

The orbital-projected DOS presented in figure 2(b,c) shows that the wide peak in Fe DOS consists of contribution from all states except that of x^2-y^2 symmetry. By contrary, in Ni DOS only the x^2-y^2 states form a peak slightly below the Fermi level.

In figure 3 we display the imaginary part of electronic self-energy $\Sigma(i\nu_n)$ as a function of fermionic Matsubara frequency ν_n . For Fe atoms, only the self-energy for x^2-y^2 states has a Fermi-liquid-like form, but indicates a small life-time of quasiparticles, which is inverse proportional to $\text{Im}\Sigma(i\nu \rightarrow 0)$. At the same time, all other states show the non-coherent behavior, which is similar to that of e_g states in bcc

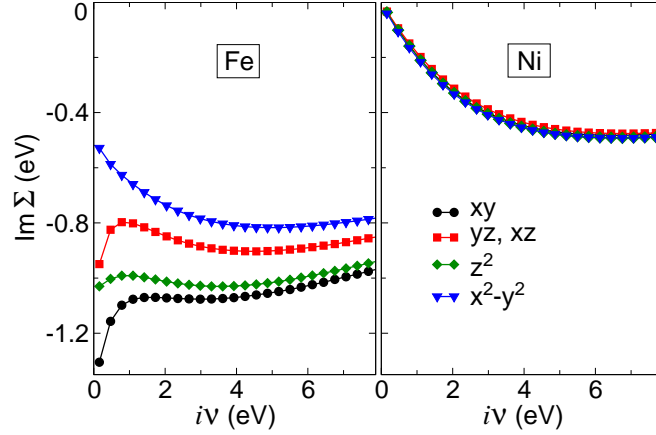


Figure 3. Imaginary part of electronic self-energy on Fe (left part) and Ni (right part) sites as a function of imaginary frequency $i\nu$ obtained by DFT+DMFT at $\beta = 20 \text{ eV}^{-1}$.

Fe [21–23], due to the above mentioned peaks of the DOS. The non-Fermi-liquid behavior is not observed in calculations with $J_H = 0$, that indicates an important role played by the Hund’s exchange. The behavior of self-energies for Ni atoms is completely different than that for Fe sites, namely, similarly to pure Ni [25], all $\Sigma(i\nu_n)$ have a Fermi-liquid form with small quasiparticle damping, indicating a presence of long-lived quasi-particles with average mass enhancement factor $m^*/m = 1.23$.

Next we calculate the uniform magnetic susceptibility, which shows Curie-Weiss behavior (see figure 4). The dominant contribution to uniform susceptibility is provided by Fe sites, while the Ni sites contribution is subleading. The Curie temperature, extracted from the linear extrapolation of inverse susceptibility is $T_C \approx 1750 \text{ K}$. Counting two times overestimation of the Curie temperature due to the Ising symmetry of Hund’s exchange and mean-field approximation (see Refs. [25, 40]), we find expected Curie temperature $\sim 850 \text{ K}$, which agrees well with the experimental data.

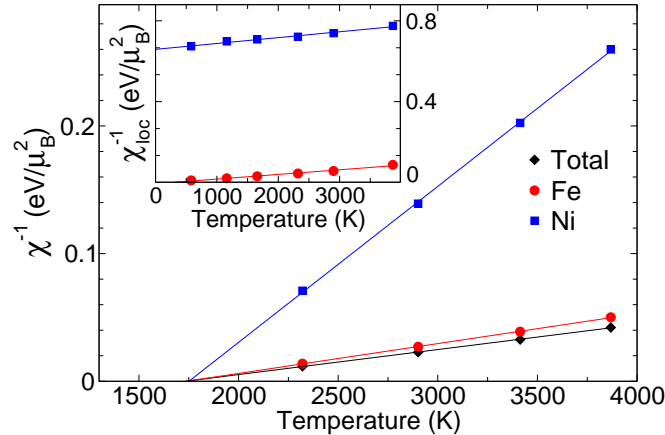


Figure 4. Temperature dependence of inverse uniform (main panel) and local (inset) magnetic susceptibility calculated by DFT+DMFT. The straight lines depict the least-squares fit to the linear dependence.

Local static susceptibility $\chi_{\text{loc}} = 4\mu_B^2 \int_0^\beta \chi_{\text{loc}}(\tau) d\tau$, where $\chi_{\text{loc}}(\tau) = \langle S_z(\tau) S_z(0) \rangle$, also shows Curie-Weiss behavior (see inset of Fig. 4) with negative Weiss temperature T_{loc} , which absolute value corresponds to the Kondo temperature T_K up to the numerical prefactor of order of one [41–43]. Similarly to bcc iron, the contribution of Fe sites is characterized by small T_K , showing well-formed local moments. On contrary, Ni sites are characterized by rather large Kondo temperature T_K , i.e. absence of local moments, which is in line with the Fermi-liquid-like self-energies for these sites.

The imaginary time dependence of the dynamic susceptibilities $\chi_{\text{loc}}(\tau) = \langle S_z(\tau) S_z(0) \rangle$ is shown in figure 5, together with the real part of $\chi_{\text{loc}}(\omega)$, obtained by Fourier transform and analytical continuation to real frequency ω using Padé approximants [37]. Fe sites are characterized by the finite broad plateau in the time dependence and sharp peak in frequency dependence, which confirms existence of well-defined local magnetic moments on these sites. The local moments disappear with switching off Hund’s exchange, that shows explicitly that the obtained peculiarities of magnetic properties of Fe sites are the characteristics of Hund’s metal behavior [44]. At the same time, Ni sites have almost vanishing correlation function at finite imaginary times $\tau \sim \beta/2$, and absent peak of the frequency dependence, independently of Hund’s exchange, showing once more the absence of local moments on these sites.

Finally we consider the particle-hole bubble (irreducible static non-uniform magnetic susceptibility)

$$\chi_{\mathbf{q}}^0 = -\frac{2\mu_B^2}{\beta} \sum_{\mathbf{k}, \nu_n, ij, m, m'} G_{\mathbf{k}}^{im, jm'}(i\nu_n) G_{\mathbf{k}+\mathbf{q}}^{jm', im}(i\nu_n), \quad (1)$$

where $G_{\mathbf{k}}^{im, jm'}(i\nu_n)$ is the one-particle Green function for d -states obtained using the Wannier-projected Hamiltonian, i, j and m, m' are the site and orbital indexes, respectively.

One can see (Fig. 6) that $\chi_{\mathbf{q}}^0$ has its maximum at Γ point ($\mathbf{q}=0$), implying

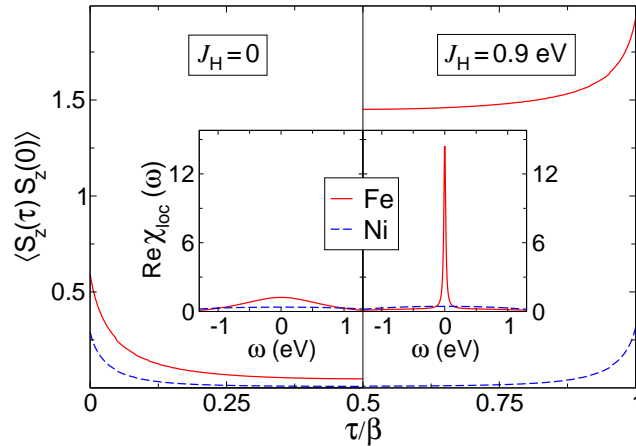


Figure 5. Local spin-spin correlation function for Fe and Ni sites in the imaginary-time (main panel) and real-frequency (inset) domains calculated by DFT+DMFT at $\beta = 10 \text{ eV}^{-1}$ with $J_H = 0$ (left part) and $J_H = 0.9 \text{ eV}$ (right part).

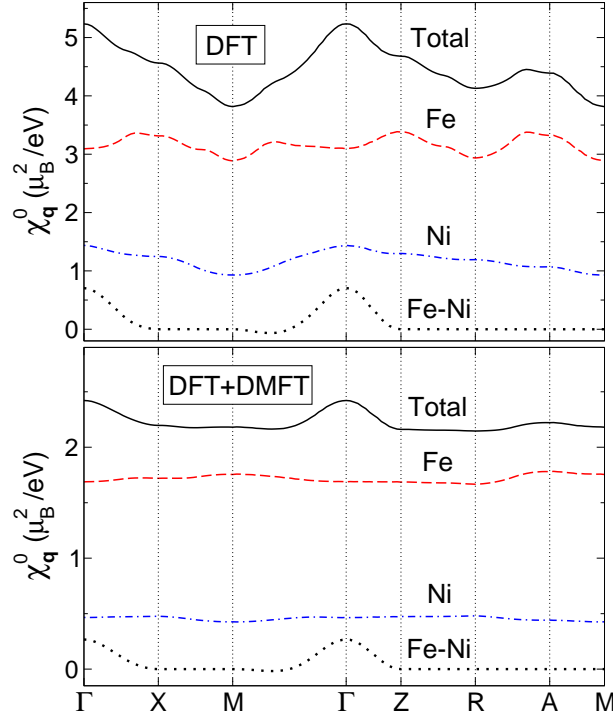


Figure 6. Momentum-dependence of the particle-hole bubble and its partial contributions from Fe and Ni sites obtained within DFT (top panel) and DFT+DMFT (bottom panel) at $\beta = 10 \text{ eV}^{-1}$.

that ferromagnetism is favoured in both DFT and DMFT approaches. However, this maximum appears mainly because of the mixed Fe-Ni contributions. At the same time, the contribution of iron sites does not favour ferromagnetism in DFT, and almost momentum-independent in DMFT, similarly to bcc iron [22]. For $L1_0$ FeNi the latter weak momentum dependence occurs since electronic states, corresponding to major part of Fe orbitals (except x^2-y^2), show the non-Fermi liquid behavior, and the main contribution to non-uniform susceptibility in DMFT is provided by mixed Fe-Ni part. This is similar to the mixed t_{2g} - e_g contribution to particle-hole bubble in bcc iron [22, 23], with t_{2g} states being more itinerant, while e_g states being more localized. Since momentum dependence of particle-hole bubble can be related to the magnetic exchange [22, 23], from these findings one can expect RKKY-type of magnetic exchange in $L1_0$ FeNi, with the states corresponding to nickel sites (including virtual hopping to iron sites) providing itinerant contribution and iron states providing local moment contribution.

4. Conclusion

Our DFT+DMFT study of $L1_0$ FeNi has revealed that magnetism of Fe and Ni sites is completely different. The former is characterized by well-defined local magnetic moments, which appear due to Hund's exchange, while the latter is much more itinerant.

Although the crystal structure is close to the fcc one, the localized magnetism and behavior of self-energy of Fe sites resemble those in pure bcc Fe. This can be explained by presence of peaks in the DOS near the Fermi level in $L1_0$ FeNi, similar to that in e_g states of bcc Fe.

The estimated Curie temperature agrees with the experimental data, up to the factor of two, which appears because of considering Ising symmetry of Hund's exchange and limitations of dynamical mean-field theory.

The calculated local magnetic susceptibility confirms different magnetic behavior of Fe and Ni sites. The obtained momentum dependence of particle-hole bubble suggests that the magnetic exchange in $L1_0$ FeNi is of RKKY-type, with iron states providing local-moment contribution, and the states corresponding to nickel sites (including virtual hopping to iron sites) providing itinerant contribution.

Therefore, $L1_0$ FeNi is a good candidate for rare-earth-free magnets. Further studies (e.g., its doping/alloying) may find the way for its better phase stability. The search of other rare-earth-free magnets will also allow one to achieve better performance characteristics, such as coercive force and magnetic energy product. Both theoretical and experimental investigations of such magnets have to be performed.

Acknowledgments

The DMFT calculations were supported by the Russian Science Foundation (project 19-72-30043). The DFT calculations were supported by the Ministry of Science and Higher Education of the Russian Federation (theme Electron No. AAAA-A18-118020190098-5).

References

- [1] Paulevé J, Dautreppe D, Laugier J and Néel L 1962 *Compt. rend. Acad. Sci.* **254** 965
- [2] Shima T, Okamura M, Mitani S and Takanashi K 2007 *J. Magn. Magn. Mater.* **310** 2213
- [3] Kojima T, Ogiwara M, Mizuguchi M, Kotsugi M, Koganezawa T, Ohtsuki T, Tashiro T Y and Takanashi K 2014 *J. Phys.: Condens. Matter* **26** 064207
- [4] Makino A, Sharma P, Sato K, Takeuchi A, Zhang Y, Takenaka K 2015 *Scientific Reports* **5** 16627
- [5] Kotsugi M, Maruyama H, Ishimatsu N, Kawamura N, Suzuki M, Mizumaki M, Osaka K, *et al* 2014 *J. Phys. Condens. Matter* **26** 064206
- [6] Lewis L H, Mubarak A, Poirier E, Bordeaux N, Manchanda P, Kashyap A, Skomski R, Goldstein J, Pinkerton F E, Mishra R K, Kubic Jr R C and Barmak K 2014 *J. Phys.: Condens. Matter* **26** 064213
- [7] Wasilewski P 1988 *Phys. Earth Planet. In.* **52** 150
- [8] Poirier E, Pinkerton F E, Kubic R, Mishra R K, Bordeaux N, Mubarak A, Lewis L H, Goldstein J I, Skomski R and Barmak K 2015 *J. Appl. Phys.* **117** 17E318
- Bordeaux N, Montes-Arango A M, Liu J, Barmak K and Lewis L H 2016 *Acta Mater.* **103** 608
- [9] Paulevé J, Chamberod A, Krebs K and Bourret A 1968 *J. Appl. Phys.* **39** 989
- [10] Néel L, Pauleve J, Pauthenet R, Laugier J and Dautreppe D 1964 *J. Appl. Phys.* **35** 873
- Chamberod A, Laugier J and Penisson J M 1979 *J. Magn. Magn. Mater.* **10** 139
- Reuter K B, Williams D B and Goldstein J I 1989 *Metall. Trans. A* **20A** 711
- Lee S, Edalati K, Iwaoka H, Horita Z, Ohtsuki T, Ohkochi T, Kotsugi M, Kojima T, Mizuguchi M and Takanashi K 2014 *Phil. Mag. Lett.* **94** 639

- [11] Mizuguchi M, Kojima T, Kotsugi M, Koganezawa T, Osaka K and Takanashi K 2011 *J. Magn. Soc. Japan* **35** 370
- [12] Frisk A, Lindgren B, Pappas S D, Johansson E and Andersson G 2016 *J. Phys.: Condens. Matter* **28** 406002
- [13] Momma K and Izumi F 2011 *J. Appl. Crystallogr.* **44** 1272
- [14] Miura Y, Ozaki S, Kuwahara Y, Tsujikawa M, Abe K and Shirai M 2013 *J. Phys.: Condens. Matter* **25** 106005
- [15] Kota Y and Sakuma A 2012 *Journal of the Physical Society of Japan* **81** 084705
- [16] Izardar A and Ederer C, *arXiv*:2003.04181
- [17] Edström A, Chico J, Jakobsson A, Bergman A and Ruzs J, 2014 *Phys. Rev. B* **90** 014402.
- [18] Tian L-Y, Levämäki H, Eriksson O, Kokko K, Nagy Á, Délczeg-Czirják E K and Vitos L 2019 *Scientific Reports* **9** 8172
- [19] Mohri T and Chen Y 2004 *J. Alloy. Comp.* **383** 23
Mohri T, Chen Y and Jufuku Y 2009 *Calphad* **33** 244
- [20] Barabash S V, Chepulskii R V, Blum V and Zunger A 2009 *Phys. Rev. B* **80** 220201(R)
- [21] Katanin A A, Poteryaev A I, Efremov A V, Shorikov A O, Skorniyakov S L, Korotin M A, Anisimov V I 2010 *Phys. Rev. B* **81** 045117
- [22] Igoshev P A, Efremov A V, Katanin A A 2015 *Phys. Rev. B* **91** 195123
- [23] Belozerov A S, Katanin A A, Anisimov V I 2017 *Phys. Rev. B* **96** 075108
- [24] Lichtenstein A I, Katsnelson M I and Kotliar G 2001 *Phys. Rev. Lett.* **87** 067205
Grechnev A, Di Marco I, Katsnelson M I, Lichtenstein A I, Wills J and Eriksson O 2007 *Phys. Rev. B* **76** 035107
Leonov I, Poteryaev A I, Anisimov V I and Vollhardt D 2011 *Phys. Rev. Lett.* **106** 106405
Benea D, Minár J, Chioncel L, Mankovsky S and Ebert H 2012 *Phys. Rev. B* **85** 085109
Leonov I, Poteryaev A I, Anisimov V I and Vollhardt D 2012 *Phys. Rev. B* **85** 020401(R)
- [25] Hausoel A, Karolak M, Şaşıoğlu E, Lichtenstein A, Held K, Katanin A, Toschi A, Sangiovanni G 2017 *Nature Communications* **8** 16062
- [26] Minár J, Chioncel L, Perlov A, Ebert H, Katsnelson M I and Lichtenstein A I 2005 *Phys. Rev. B* **72** 045125
- [27] Leedahl B *et al* 2016 *RSC Adv.* **6** 85844
- [28] Metzner W and Vollhardt D 1989 *Phys. Rev. Lett.* **62** 324
Georges A, Kotliar G, Krauth W and Rozenberg M J 1996 *Rev. Mod. Phys.* **68** 13
- [29] Anisimov V I, Poteryaev A I, Korotin M A, Anokhin A O and Kotliar G 1997 *J. Phys. Condens. Matter* **9** 7359
Kotliar G, Savrasov S Y, Haule K, Oudovenko V S, Parcollet O and Marianetti C A 2006 *Rev. Mod. Phys.* **78** 865
Kuneš J, Leonov I, Augustinský P, Krápek V, Kollar M and Vollhardt D 2017 *Eur. Phys. J. Special Topics* **226** 2641
- [30] Benea D, Minár J, Ebert H and Chioncel L 2018 *Phys. Rev. B* **97** 144408
- [31] Haule K 2007 *Phys. Rev. B* **75** 155113
Pourovskii L V, Amadon B, Biermann S, and Georges A 2007 *Phys. Rev. B* **76** 235101
Amadon B, Lechermann F, Georges A, Jollet F, Wehling T O and Lichtenstein A I 2008 *Phys. Rev. B* **77** 205112
Aichhorn M, Pourovskii L, Vildosola V, Ferrero M, Parcollet O, Miyake T, Georges A and Biermann S 2009 *Phys. Rev. B* **80** 085101
- [32] Baroni S, de Gironcoli S, Dal Corso A and Giannozzi P 2001 *Rev. Mod. Phys.* **73** 515
Giannozzi P, Baroni S, Bonini N, Calandra M, Car R, Cavazzoni C, Ceresoli D, Chiarotti G L, Cococcioni M, Dabo I *et al* 2009 *J. Phys.: Condens. Matter* **21** 395502
- [33] Leonov I, Binggeli N, Korotin Dm, Anisimov V I, Stojić N and Vollhardt D 2008 *Phys. Rev. Lett.* **101** 096405
Leonov I, Korotin Dm, Binggeli N, Anisimov V I and Vollhardt D 2010 *Phys. Rev. B* **81** 075109

- [34] Marzari N, Mostofi A A, Yates J R, Souza I and Vanderbilt D 2012 *Rev. Mod. Phys.* **84** 1419
- [35] Belozarov A S and Anisimov V I 2014 *J. Phys.: Condens. Matter* **26** 375601
- [36] Rubtsov A N, Savkin V V and Lichtenstein A I 2005 *Phys. Rev. B* **72** 035122
Werner P, Comanac A, de Medici L, Troyer M and Millis A J 2006 *Phys. Rev. Lett.* **97** 076405
- [37] Vidberg H J and Serene J W 1977 *J. Low Temp. Phys.* **29** 179
- [38] Igoshev P A, Efremov A V, Poteryaev A I, Katanin A A, Anisimov V I 2013 *Phys. Rev. B* **88** 155120
- [39] Guillot C, Ballu Y, Paigne J, Lecante J, Jain K P, Thiry P, Pinchaux R, Petroff Y and Falicov L M 1977 *Phys. Rev. Lett.* **39** 1632
- [40] Belozarov A S, Leonov I and Anisimov V I 2013 *Phys. Rev. B* **87** 125138
- [41] Wilson K 1975 *Rev. Mod. Phys.* **47** 773
- [42] Mel'nikov V I 1982 *Soviet Phys. JETP Lett.* **35** 511
- [43] Tsvelick A M and Wiegmann P B 1983 *Adv. Phys.* **32** 453
- [44] Yin Z P, Haule K and Kotliar G 2011 *Nat. Mater.* **10** 932
de'Medici L, Mravlje J and Georges A 2011 *Phys. Rev. Lett.* **107** 256401
Belozarov A S, Katanin A A and V. I. Anisimov *Phys. Rev. B* 2018 **97**, 115141
Werner P, Gull E, Troyer M, and Millis A J 2008 *Phys. Rev. Lett.* **101** 166405